Article

Characterization of Photothermal Desorption-Compatible Diffusive Samplers for Volatile Organic Compounds

Jacob S. Shedd, Jonghwa Oh, Evan L. Floyd, and Claudiu T. Lungu*

Cite This: ACS Environ. Au 2023, 3, 242−248

Read Online

ACCESS | 📊 Metrics & More | 📖 Article Recommendations | 🆂🅸 Supporting Information

ABSTRACT: Products and starting materials containing volatile organic compounds (VOCs) can easily be found in a variety of businesses, making them a common source of occupational exposure. To prevent negative impacts on employee health, field industrial hygienists must conduct regular sampling to ensure exposures remain below the regulatory limits set by governmental and professional associations. As such, the need for sensitive and reliable exposure assessment techniques becomes evident. Over the preceding decade, the industrial hygiene research group at the University of Alabama at Birmingham (UAB) has been working on the development of an emerging, preanalytical technique known as photothermal desorption (PTD) to improve upon the analytical sensitivity of currently employed methods. PTD's novel design uses pulses of high-energy light to desorb analytes from thermally conductive, carbonaceous sorbents, to be delivered to downstream analytical detectors. Since PTD's conception, the theoretical framework and advances in sorbent fabrication have been investigated; however, further work is needed to produce a field-ready sampling device for use with PTD. As such, objectives of the present work were to design a PTD-compatible diffusive sampler prototype and characterize the prototype's sampling efficiencies for toluene, *n*-hexane, trichloroethylene, and isopropyl alcohol. In pursuit of these objectives, the study empirically quantified the sampled masses of toluene, *n*-hexane, trichloroethylene, and isopropyl alcohol, at occupationally relevant air concentrations, to be 12.17 ± 0.06, 8.2 ± 0.1, 3.97 ± 0.06, and 8.0 ± 0.1 mg, respectively. Moreover, the analyte sampling efficiencies were found to be 2.2 ± 0.1, 1.7 ± 0.1, 1.2 ± 0.1, and 0.51 ± 0.05 (unitless) when comparing empirically (i.e., laboratory observed) sample mass values to theoretically predicted values. The sampling efficiencies and collected sample masses reported herein demonstrate the promising design of PTD-compatible diffusive samplers. When used in conjunction with the PTD method, the prototype samplers present strong evidence for improving analytical sensitivity in exposure assessments of VOCs in the workplace.

KEYWORDS: volatile organic compounds, exposure assessment, diffusive sampling, gas chromatography, method development, industrial hygiene, photothermal desorption
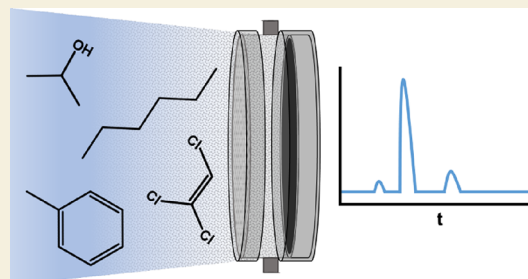
1. INTRODUCTION

Frequently seen in solvents, degreasers, cleansers, adhesives, petroleum distillates, and many other goods, exposure to VOCs places millions of workers[1] at risk of developing a range of adverse health effects, including mucosal membrane irritation, kidney and liver damage, temporary and permanent central nervous system effects, cancer, and death.[2−4] In an effort to prevent the occurrence of these effects, professional associations[5,6] and regulatory bodies[7] developed occupational exposure limits (OELs) to be used as safeguards in the workplace. Traditionally, OEL compliance has been verified by collecting personal air samples from potentially exposed employees via sorbent tubes with battery-powered sampling pumps attached as a means of pulling air through the sampling train. Considering the potential for electronic failures and the cumbersome nature of sampling trains, a viable alternative can be found in the use of diffusive samplers—compact and lightweight sampling devices that rely on down-gradient diffusion to passively collect volatile

analytes—as a convenient means for conducting sampling. However, diffusive samplers present limitations particularly when it comes to analytical sensitivity. Relying on the process of diffusion results in lowered mass uptake rates; the collected mass is then further reduced by up to 1000× via dilution with extraction solvents (e.g., chemical desorption; CD)[8−12] and aliquot injection into a gas chromatograph (GC) for sample quantification. This ultimately means that diffusive sampling is limited in its ability to collect an analytically relevant sampling mass during short sample periods (i.e., <8 h) or when sampling for low-concentration VOCs.

Over the last decade, the industrial hygiene research group at the University of Alabama at Birmingham (UAB) has been striving to address the limitations of diffusive samples through the development of the novel, preanalytical method known as photothermal desorption (PTD). This emerging technique uses flashes of visible light to desorb VOC analytes collected on thermally conductive sorbents (i.e., buckypapers; BPs) fabricated from single-walled carbon nanotubes (SWNTs).[13−18] Since PTDs were first introduced,[13] the method and sorbents have been refined and characterized.[14−17,19] However, to further develop PTD into a commercial-ready sampling and analysis method, a compatible diffusive sampler should be designed to house BPs during sample collection and desorption. Steps toward the development of prototype samplers have been made in a study concerning the ability of commercially available, stainless steel meshes to be used as prototype windscreens.[18] Still, a fully developed PTD-compatible sampler has yet to come to fruition.

To address this gap, our team has designed and fabricated a first-generation PTD-compatible sampler prototype for use in collection and PTD of a variety of VOC analytes. In the present study, existing analytical methods from the National Institute of Occupational Safety and Health (NIOSH; Methods 1401[12] and 1501[9]) were adapted for the purpose of empirically characterizing the sampling efficiencies of the prototype samplers for toluene, n-hexane, trichloroethylene (TCE), and isopropyl alcohol (IPA). This objective was achieved by exposing PTD-compatible samplers to the respective 8 h threshold limit values (TLV_{8-hr})[20−23] for each analyte of interest, generated in a dynamic sampling chamber, over a period of 8 h.

2. METHODS

2.1. Buckypaper Fabrication

Arc-discharge (AD) SWNTs (94.5% pure, 1.2−1.7 nm diameter, 0.1−4 μm length) were purchased presuspended from Nanointegris Inc. (Quebec, Canada) and used for the fabrication of self-supporting buckypaper sorbents. To maintain consistency with our previous works,[14−16,19] 50 mL of the SWNT solution was combined, as obtained, with 400 mL of ACS grade acetone and allowed to sit overnight (~15 h). The resulting solution was then vacuum filtered against a polytetrafluoroethylene membrane filter (47 mm diameter, 5 μm pore size, EMD Milipore, Darmstadt, Germany), immediately followed by 30 min of vacuum drying and a repeated, two-step cleaning cycle comprising a 250 mL rinse with H_2O (HPLC grade) and a 40 mL rinse with acetone. After rinsing, the SWNT cake was vacuum-dried for 30 min followed by an additional 2 h of air drying. The completed BPs was then delaminated from the membrane filter and heat-treated at 300 °C for 90 min using a muffle furnace (Thermolyne F48025-60-80, Thermo Fisher Scientific, Waltham, MA) with temperature ramping set to 10 °C/min.[15] BPs were then placed in 100 °C storage until used in sample collection.

2.2. PTD-Compatible Diffusive Sampler Design

First-generation prototype samplers were drafted using AutoCAD (Autodesk; San Rafael, CA; Drafted by Creative Engineering, Bronxville, NY) and fabricated from nylon 6,6 via computer numerical control (CNC) machining (Manufactured by Xometry, Gaithersburg, MD). Our first-generation design was similar to other commercially available organic vapor monitors, with key modifications to integrate the sampler with a PTD system. The sampler design shown in Figure 1 is two-sided with a diffusion path length of 1 cm. The top side allows analyte diffusion through a stainless-steel mesh windscreen (pore diameter: 0.014 cm; open area: 30%; McMaster-Carr; Elmhurst, IL) to a BP sorbent where analyte is collected via adsorption. On the reverse side (bottom) of the sampler, the BP rests against a quartz glass window (diameter: 3.81 cm; thickness: 0.32 cm; McMaster-Carr; Elmhurst, IL),
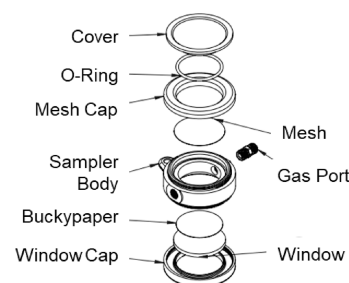
Figure 1. Schematics of a first-generation prototype diffusive sampler for use with PTD. The two-sided design allows analyte adsorption on the top side and PTD on the reverse.

allowing visible light irradiation. In addition, 0.32 cm (inner diameter) brass fittings were threaded into the sampler side walls to allow N_2 (g) to flow through the sampler during sample analysis. The fittings could then be capped during sampling to prevent disturbances in the diffusion gradient by closing the system.

2.3. Equipment Calibration

2.3.1. Photoionization Detector Calibration. A 10.6 eV photoionization detector (PID; range: 0.1−2000 ppm) was obtained from Baseline-Mocon (VOC-Traq II; Lyons, CO) and calibrated weekly using a 2-point calibration (zero gas: dry N_2; span gas: 100 ppm isobutylene in N_2), as prescribed by the manufacturers.[24] Data was monitored using VOC-Traq II software (v. 1.0.0.32).

2.3.2. Gas Chromatograph Calibration. A 6-point calibration curve was used to calibrate a GC with flame-ionization detector (GC-FID; Model 6850, Agilent Technologies, Santa Clara, CA) for toluene (ACS grade; range: 103.5−2586.7 μg/mL; r^2 = 0.99991), n-hexane (99 + %; range: 97.8−1711.0 μg/mL; r^2 = 0.99976), TCE (99.9%; range: 207.0−5173.8 μg/mL; r^2 = 0.99977), and IPA (99.9%; range: 448.4−11,210 μg/mL; r^2 = 0.99438) in CS_2 (ACS grade; internal standard: 50 μg/mL 4-chlorobenzotrifluoride); all solvents were sourced from Fisher Scientific (Waltham, MA). GC-FID analytical conditions were adopted and modified from National Institute of Occupational Health and Safety (NIOSH) method 1501[9] for toluene, n-hexane, and TCE (i.e., inlet: 250 °C; oven/column: 70 °C for 0.5 min and 190 °C for 2.5 min, ramping rate 60 °C/min; detector: 250 °C) and NIOSH method 1401[12] for IPA (i.e., inlet 250 °C; oven/column: 70 °C for 3 min; detector: 250 °C). The GC auto-injector was cleaned between each analyte injection using IPA. A low polarity, fused silica column (J&W HP-1 GC Column; 30 m × 0.32 mm × 0.25 μm; Agilent Technologies, Santa Clara, CA) was used with each analyte, and the in situ FID was assumed to have a mass flow of <1.4 pgC/s (using tridecane) and a linear dynamic range of >107 (±10%), per the manufacturer's technical data.[25] Calibration curves and regression equations for each analyte can be obtained from Appendix B of the supplied Supporting Information.

2.4. Dynamic Exposure Chamber

A 2.5 L (1152 in³) aluminum exposure chamber was fabricated by UAB's Research Machine Shop. The chamber was engineered to promote analyte/air mixing via the inclusion of a stainless-steel mesh (open area: 22%) and designed to hold four diffusive samplers simultaneously at various heights (i.e., 18.7, 21.4, 25.4, and 27.5 cm) as seen in Figure 2. To create a consistent gas flow within the chamber, compressed air was generated in a 96 L air compressor (Kobalt Quiet Tech; Lowe's Companies, Inc.; Mooresville, NC) and flowed through an anhydrous $CaSO_4$ desiccant and water trap to remove liquid H_2O from the airstream (RH = 51% after drying) prior to entering a mass-flow controller (rang: 0−100 SLPM; Sierra Instruments; Monterey, CA). A pressure of approximately 827.4 kPa (~120 psi) was applied to a mass-flow controller to deliver a flow rate (Q) of 74 L/min to the exposure chamber with cross sectional area of 412.9 cm². The addition of a cross flow mixing mesh further decreased the cross-sectional area to 90.8 cm² allowing for a sampler face velocity of 26.5 ft/min to be generated. VOC analytes were introduced into the gas flow via an injection port installed before the exposure chamber, and a program-
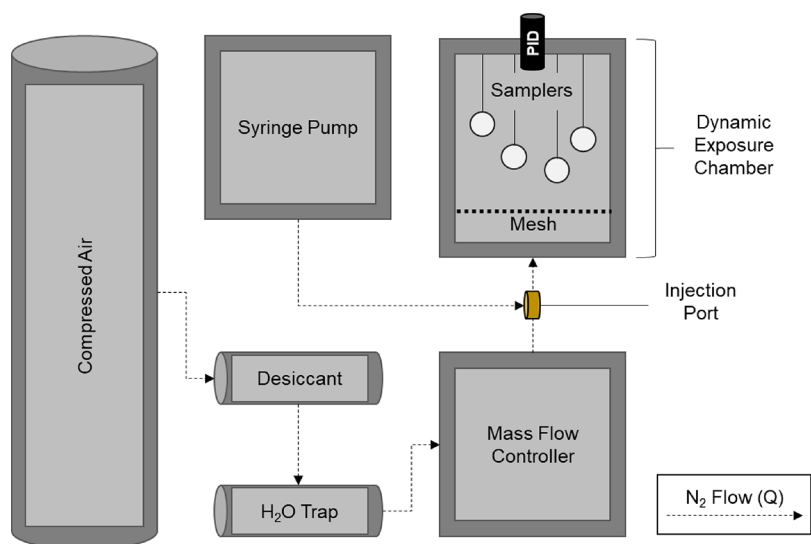
Figure 2. Flow diagram of the dynamic exposure chamber used for analyte dosing.

mable syringe pump (Model: F100X; Chemyx; Stafford, TX) was used to maintain a constant concentration within the chamber.

To collect samples for a given analyte, four prototype samplers (samplers 1–4) were hung in the exposure chamber with their mesh diffusion barriers facing inward and were exposed to the analyte of interest for 8 h. Analyte concentrations of occupational relevance were generated within the chamber at or near the permissible exposure limits (PELs) prescribed by the Occupational Safety and Health Administration (OSHA) for the respective chemical under investigation (toluene: 200 ppm, n-hexane: 200 ppm, TCE: 100 ppm, IPA: 400 ppm)[25−28] and verified in real-time via an in-line PID inserted at a depth of 25.4 cm from the chamber lid.

2.5. Chemical Desorption & Gas Chromatography

At the conclusion of each sample collection run, the dosed BPs were removed from their respective sampler bodies and placed into glass jars (volume = 40 mL) for desorption. To extract analytes from the BPs, 5 mL of CS_2 was added to each jar to enable chemical desorption. The jars were then capped, and the BPs were allowed to desorb for 30 min prior to filtering (syringe filter; Millex-HV; 0.45 μm; Millipore, Bedford, MA) and storing the analyte/CS_2 solution at 5 °C (storage time: 24–48 h) to maintain sample integrity for GC analysis.

GC analysis was performed using the analytical conditions and instrumentation described in the preceding Gas Chromatograph Calibration section. Approximately 150 μL of analyte/CS_2 solution from each sampler is transferred into a GC autosampler vial (ThermoFischer Scientific, Co; Waltham, MA) for a given analyte, and a 1 μL aliquot was injected into the GC-FID from each sample. This procedure was performed in triplicate for all samplers, and the resulting data were averaged by analyte of interest (i.e., toluene, n-hexane, TCE, and IPA). Samples were assumed to be free of contamination if no observable elution peaks were detected aside from those associated with the analyte being investigated during a given analytical run. Representative chromatograms for each analyte can be obtained from Appendix B of the provided Supporting Information.

2.6. Determination of Analyte Uptake Rates

2.6.1. Theoretical Sampling Rate Calculation. The binary diffusion coefficients for toluene, n-hexane, TCE, and IPA in air were calculated based on the Fuller, Schettler, and Giddings equation (eq 1).[26,27] Equation 2[28,29] was then used to determine the theoretical uptake rate of the samplers based on the results of eq 1 and the diffusive sampler's geometry.

$$D_{AB} = \frac{1.00 \times 10^{-3} \times T^{1.75} \times (1/M_A + 1/M_B)^{1/2}}{\rho[\sum_A v_i^{1/3} + \sum_B v_i^{1/3}]^2} \quad (1)$$

where D_{AB} is the binary diffusion coefficient (cm²/s) of compound A in compound B (i.e., air), T is the absolute temperature (K; room temperature: 273.15 K), M_A and M_B are the respective molecular weights of compounds A and B, ρ is the atmospheric pressure (atm); $\sum_A v_i$ and $\sum_B v_i$ are the atomic diffusion volumes, and v_i is a dimensionless diffusion parameter to be summed over atoms, functional groups, and structural features of the diffusing species (Table 1).

$$UR_{ideal} = \frac{D_{AB} \times A}{L} \times 60 \quad (2)$$

Table 1. Atomic Diffusion Volumes[27,30]

atomic and structural diffusion volume increments (v_i)			
C	15.9	Cl	21.0
H	2.31	aromatic or heterocyclic ring	−18.3
O	6.11		
diffusion volumes of atoms and simple molecules ($\sum v_i$)			
air		19.7	

where UR_{ideal} is the theoretically calculated, sampler uptake rate (cm³/min) of compound A in compound B (i.e. air), A is the cross-sectional area of the diffusion path (prototype: A = 2.724 cm²), L is the diffusive path length (prototype: L = 1 cm), and 60 is the conversion coefficient from cm³/s to cm³/min.

2.6.2. Effective Uptake Rate Determination. The effective (actual) uptake rate for each analyte of interest was determined using eq 3, based on empirically measures values such as the sampling period, the sample extraction volume, the chamber concentration, and the sample concentration as determined by the GC elution curve area and calibration equation. The derivation of this equation can be seen in the Supporting Information provided.

$$UR_{eff} = \frac{C_{GC} \times V_{extraction}}{t \times C_{chamber} \times 10^{-3}} \quad (3)$$

where UR_{eff} is the effective, sampler uptake rate (cm³/min), C_{GC} is the empirically measured concentration (μg/mL) via GC, within the analyte extraction solution, $V_{extraction}$ is the volume of CS_2 used to extract the sample from the sorbent (5 mL), t is the sampling period in minutes, $C_{chamber}$ is the empirically measured concentration (mg/m³) within the exposure chamber, and 10^{-3} is the conversion coefficient for mg/m³ to μg/mL.

2.6.3. Calculating Sampling Efficiency. The sampling efficiency (α) of each analyte was derived from the work of Jia and Fu in 2017,[29] resulting in the following expression (eq 4), which relates sampling efficiency in terms of uptake rate, air volume sampled, and mass sampled. The derivation of this equation can be found in the Supporting Information provided.

$$\alpha = \frac{UR_{eff}}{UR_{ideal}} = \frac{V_{eff}}{V_{ideal}} = \frac{m_{eff}}{m_{ideal}} \qquad (4)$$

where UR_{eff} and UR_{ideal} are the effective and theoretical uptake rates (cm^3/min) respectively, V_{eff} and V_{ideal} are the effective and theoretical volumes of air collected by the sampler (cm^3), and m_{eff} and m_{ideal} are the effective and theoretical sample masses collected by the sampler (μg), respectively.

3. RESULTS

The data presented in Table 2 depicts the exposure chamber conditions (i.e., sampling duration and analyte concentration)

Table 2. GC Concentrations of Analytes Extracted from Prototype Samplers Via Chemical Desorption

	exposure chamber			
analyte	time (h)	C_{PID} (mg/m^3)^{a,b}	$V_{extraction}$ (mL)	C_{GC} (μg/mL)^{b,c}
toluene	8.0	890 ± 100	5	2434 ± 137
n-hexane	8.0	815 ± 101		1638 ± 101
trichloroethylene	8.0	542 ± 94		794 ± 31
2-propanol	8.0	1963 ± 338		1593 ± 136

^{a}Chamber concentration from in situ PID. ^{b}Values written as "average ± STDEV". ^{c}n = 12.

during analyte sample collection, and the average concentrations of sampled analyte after extraction with 5 mL of CS_2, as quantified by GC. Table 3 shows the theoretical and empirically

Table 3. Comparison of Theoretical (m_{ideal}) and Empirically Collected (m_{eff}) Analyte Sample Masses and the Resulting Sampling Efficiency (α)

analyte	m_{ideal} (mg)^a	m_{eff} (mg)^{a,b}	$\alpha^{a,b}$
toluene	5.5 ± 0.6	12.17 ± 0.06	2.2 ± 0.1
n-hexane	4.8 ± 0.6	8.2 ± 0.1	1.7 ± 0.1
trichloroethylene	3.4 ± 0.06	3.97 ± 0.06	1.2 ± 0.1
2-propanol	15.5 ± 2.7	8.0 ± 0.1	0.51 ± 0.05

^{a}Values written as "average ± error". ^{b}n = 12.

determined analyte masses collected by the sampler prototypes, and the sampling efficiency of the sampler for each analyte. Using theoretical uptake rates calculated via the Fuller, Schettler, and Giddings equation (eq 1)[26,27] and eq 2[28,29] and the respective C_{PID} values (Table 2), the theoretical masses (m_{ideal}) collected for toluene, n-hexane, TCE, and IPA were determined to be 5.5 ± 0.6, 4.8 ± 0.6, 3.4 ± 0.06, and 15.5 ± 2.7 cm^3/min, respectively. Empirically collected analyte masses (m_{eff}), as determined by chemical desorption and GC analysis, were observed to be 12.17 ± 0.06, 1.7 ± 0.1, 1.2 ± 0.1, and 0.51 ± 0.05 mg for toluene, n-hexane, TCE, and IPA, respectively. As reported in Table 3, the theoretical and empirically determined uptake rates were compared using eq 4 and resulted in the unitless sampling efficiencies of 2.2 ± 0.1, 1.7 ± 0.1, 1.2 ± 0.1, and 0.51 ± 0.05 for toluene, n-hexane, TCE, and IPA, respectively.

4. DISCUSSION

Table 3 data demonstrates the empirically observed sampled analyte masses (m_{eff}) of our prototype design, in comparison to the theoretical sampled masses (m_{ideal}) predicted by eqs 1 and 2 and the C_{PID} values measured within the sampling chamber (Table 2). Using eq 4 to determine sampling efficiencies (α), it can be seen that both toluene and n-hexane have collected analyte masses nearly double that of the theoretically predicted value ($\alpha_{toluene}$ = 2.2 ± 0.1; $\alpha_{n\text{-}hexane}$ = 1.7 ± 0.1), while the empirically collected mass of TCE showed a near 1:1 agreement with its corresponding theoretically predicted mass (α_{tce} = 1.2 ± 0.1). In contrast, the Table 3 data for IPA shows the empirically sampled mass of IPA to be approximately half that of the theoretically predicted mass for the analyte (α_{ipa} = 0.51 ± 0.05). In an attempt to elaborate on the discrepancies between the ideal (m_{ideal}) and effective masses (m_{eff}) reported in Table 3, this section discusses potential explanations for the deviations observed between measured and modeled sample mass, while also validating the model usage with the presented data (Table 4).

Table 4. Comparison of Reported and Calculated Sampling Rates for 3 M 3500+ Samplers^a

analyte	3500+ $Q_{reported}$ (cc/min)	3500+ Q_{est} (cc/min)	%$_{diff}$
toluene	9.48	9.47	−0.1
n-hexane	9.88	9.00	−8.9
TCE	8.60	9.67	12.5
2-propanol	11.80	12.04	2.0

^{a}$Q_{Reported}$ is the manufacturer provided flow rate, Q_{calc} is the calculated flow rate, and %$_{diff}$ is the percent difference in Q-values.

Considering that our samplers depend on physical adsorption of analytes onto the BP sorbents housed within the device, the observed discrepancies in sampling efficiency can likely be attributed to the affinity of each analyte for the BP. As analyte molecules interact with the nonuniform, porous surface of the BP, the adsorption sites on the sorbent's surface exert weak intermolecular forces on the analyte.[31−34] Depending on the analyte, these forces may or may not be sufficiently strong enough to secure analyte molecules onto the surface of the BP. Regarding the analytes investigated in the present work, toluene and n-hexane should both experience London dispersion forces as these analytes and the SWNTs making up each BP are nonpolar. In addition, toluene likely also experiences π−π interactions between the π-orbitals of the SP^2 hybridized carbon atoms in the analyte molecule and the BP. In contrast, TCE and IPA likely experience dipole-induced dipole interactions when in proximity to the BP surface, as the polar analytes induce a temporary dipole moment within the sorbent matrix. Dipole-induced dipole interactions largely depend on the polarizability of the nonpolar compound.[35] With this in mind, it is entirely possible that SWNTs within the BP are capable of producing a sufficient dipole moment to strongly adsorb nonpolar analytes while being comparatively lower than the attractive force required to strongly adsorb polar compounds. From this assumption, future studies may find it beneficial to functionalize BPs to increase their affinity for polar analytes.

Though the affinity of analytes is a fitting assumption for the sampling efficiencies observed in this study, it is also worth noting that the column used in GC analysis was specifically designated for use with low-polarity hydrocarbons. This may

cause resolution issues in the GC peaks that result in an underestimation of the m_{eff} and ultimately the sampling efficiency values reported for IPA. This seems particularly likely to be the case for the observed IPA data, as the elution peaks for this analyte were often close to the solvent (i.e., CS_2) peaks, and in some cases, minor overlap was observed between the CS_2 and IPA peaks. Reducing the GC oven temperature to 70 °C—as reflected in the Effective Uptake Rate Determination subsection of the methods—was noted to increase the resolution of the IPA and CS_2 peaks. However, despite multiple calibration runs, the r^2 for the IPA calibration curve never reached a fit above 0.99438, indicating that there may be an issue of compatibility between the analyte and the column. After consulting with the column manufacturer, it was suggested to run the column at a temperature of 40 °C for 5 min to allow for an extended retention time. This was followed by a temperature ramp to 120 °C (rate: 60 °C/min), holding at temperature for an additional 5 min, to fully purge the column. Moreover, the GC auto-injector cleaning solvent was changed to acetone in hope of reducing falsely inflated IPA elution peaks due to syringe cleaning. Taking these additional steps provided increased resolution in IPA elution peaks and showed evidence of co-elution between IPA and acetone. Co-elution was also noted when trying dichloromethane as the cleaning solvent. However, the resolution of the co-eluted peaks (i.e., IPA:acetone and IPA:dichloromethane) were not distinct enough to integrate the area under the respective curves, and as a result, the areas were summed as one. Considering the observed peak areas of cleaning solvents were relatively small compared to the IPA peaks and that IPA samples analyzed at lower temperatures were very similar to the data acquired using a column temperature of 70 °C for 3 min, the data collected from the 70 °C column was chosen as the representative data for the present work. As such, the IPA data is limited by the column selected and the slight area increase from the use of IPA as a cleaning solution.

It is worth noting that the theoretically calculated sampling rates of the prototype samplers were observed to be similar to, if not higher than the rates reported by the manufacturers of the 3 M OVM 3500+,[36] an equivalent, commercially available sampler design (Tables 4 and 5). Moreover, these design similarities

Table 5. Comparison of Sampling/Uptake Rates for 3 M 3500+ and PTD-Compatible Samplers

analyte	3500+ $Q_{reported}$ (cc/min)	UR_{ideal} (cc/min)	UR_{eff} (cc/min)[a,b]
toluene	9.48	12.96	28 ± 2
n-hexane	9.88	12.32	21 ± 1
TCE	8.6	13.24	15 ± 1
2-propanol	11.8	16.47	8.5 ± 0.7

[a]Values written as "average ± error". [b]n = 4; $Q_{Reported}$ is the manufacturer provided flow rate for the 3500+; UR_{ideal} and UR_{eff} are the theoretically and empirically determined uptake rates of PTD-compatible samplers, respectively.

were exploited to validate the use of eq 1 and eq 2 for calculating prototype sampling rates. This was achieved by applying eq 4 to manufacturer-provided specifications of the 3500+ (i.e., cross-sectional area: 0.60 cm² and diffusion path length: 0.30 cm) and the calculated binary diffusion coefficients for each analyte. Sampling rate estimates (Q_{est}) for the 3500+ using eq 2 were comparable to the manufacturer-reported sampling rate ($Q_{Reported}$), as seen in Table 4. The comparison of the reported

and calculated sampling rates resulted in percent differences ($\%_{diff}$) ranging from −8.9 to 12.5%, with all analytes but TCE falling within a percent difference of ±10%. This trend is in agreement with the manufacturer's claims that some reported sampling rates for the 3500+[36] were empirically determined, while others were calculated. Considering this information, it becomes clear that the lower the observed percent difference, the higher the probability that the reported value was calculated. From this line of thought, we concluded that the use of the Fuller, Schettler, and Giddings equation was appropriate.

5. CONCLUSIONS

The present work sought to characterize the analyte uptake rates and sampling efficiencies of a PTD-compatible diffusive sampler. This was accomplished by dosing the samplers with known concentrations of analyte and quantifying the collected analyte mass using GC. The study found the samplers collected samples masses of 12.17 ± 0.06 mg for toluene, 8.2 ± 0.1 mg for n-hexane, 3.97 ± 0.06 mg for TCE, and 8.0 ± 0.1 mg for IPA. Additionally, the present work observed analyte sampling efficiencies 2.2 ± 0.1, 1.7 ± 0.1, 1.2 ± 0.1, and 0.51 ± 0.05 for toluene, n-hexane, TCE, and IPA, respectively. This data provides strong insights into the ability of the PTD-compatible diffusive sampler to collect volatile analytes with a wide range of polarities. Moreover, the data presented herein provides strong pilot data to support future developments of PTD as a robust method for sampling and analysis.

■ ASSOCIATED CONTENT

Data Availability Statement

The authors confirm that the data supporting the findings of this study are available within the article itself. Additional questions concerning the data presented may be addressed to the corresponding author [C.T.L.].

ⓈI Supporting Information

The Supporting Information is available free of charge at https://pubs.acs.org/doi/10.1021/acsenvironau.2c00071.

> Derivations for eqs 2 and 3 (Appendix A), as well as GC calibration and chromatographic data (Appendix B) (PDF)

■ AUTHOR INFORMATION

Corresponding Author

Claudiu T. Lungu − *Department of Environmental Health Sciences, University of Alabama at Birmingham, Birmingham, Alabama 65233, United States;* ⓘ orcid.org/0000-0001-8777-1649; Email: clungu@uab.edu

Authors

Jacob S. Shedd − *Department of Environmental Health Sciences, University of Alabama at Birmingham, Birmingham, Alabama 65233, United States;* ⓘ orcid.org/0000-0003-4780-3399

Jonghwa Oh − *Department of Environmental Health Sciences, University of Alabama at Birmingham, Birmingham, Alabama 65233, United States*

Evan L. Floyd − *Department of Occupational and Environmental Health, University of Oklahoma, Oklahoma City, Oklahoma 73126, United States*

Complete contact information is available at:
https://pubs.acs.org/10.1021/acsenvironau.2c00071

Author Contributions

■ ABBREVIATIONS

VOCs	volatile organic compounds
PTD	photothermal desorption
OELs	occupational exposure limits
CD	chemical desorption
GC	gas chromatography
UAB	University of Alabama at Birmingham
BP	buckypaper
SWNTs	single-walled carbon nanotubes
NIOSH	National Institute of Occupational Safety and Health
TCE	trichloroethylene
IPA	isopropyl alcohol
TLV8-hr	8-hour threshold limit value
AD	arc discharge
CNC	computer numerical control
PID	photoionization detector
GC-FID	gas chromatograph with in-line flame ionization detector
PEL	personal exposure limit
OSHA	Occupational Safety and Health Administration

■ REFERENCES

(1) US Bureau of Labor Statistics. *Labor force statistics from the current population survey*. https://www.bls.gov/cps/lfcharacteristics. htm#occind. Published 2021. Accessed June 2, 2021.

(2) ASTDR. *INTERACTION PROFILE FOR: Benzene, Toluene, Ethylbenzene, and Xylenes (BTEX) Department of Health and Human Services Public Health Service Agency for Toxic Substances and Disease Registry*. 2004;(May). https://www.atsdr.cdc.gov/interactionprofiles/ IP-btex/ip05.pdf. Accessed January 23, 2019.

(3) WHO Working Group. *Updating and revision of the quality quidelines for Europe: report on WHO Working Group on Volatile Organic Compounds*, Brussels, Belgium, 2−6 October 1995. 1996. http://apps. who.int/iris/bitstream/handle/10665/107551/EUR_ICP_EHAZ_ 94_05_MT_12.pdf?sequence=1&isAllowed=y. Accessed April 23, 2018.

(4) U.S. EPA. *Compendium of Methods for the Determination of Toxic Organic Compounds in Ambient Air*. 2nd ed. Cincinnati; 1999. https:// www3.epa.gov/ttnamti1/files/ambient/airtox/tocomp99.pdf. Accessed October 11, 2017.

(5) National Institute for Occupational Safety and Health (NIOSH). *NIOSH Pocket Guide to Chemical Hazards*. https://www.cdc.gov/ niosh/npg/default.html. Accessed June 22, 2021.

(6) American Conference of Gonvernmental Industrial Hygienists (ACGIH). *2019 TLVs and BEIs*. Cincinnati: ACGIH S ignature Publications; 2019.

(7) Occupational Safety and Health Administration. *29 CFR* 1910. https://www.osha.gov/laws-regs/regulations/standardnumber/1910. Accessed June 22, 2021.

(8) National Institute for Occupational Safety and Health (NIOSH). Hydrocarbons, BP 36°-216°C: Method 1500. *NIOSH Man Anal Methods*. **1994**, 8−11. https://www.cdc.gov/niosh/docs/2003-154/ pdfs/1500.pdf

(9) National Institute for Occupational Safety and Health (NIOSH). Hydrocarbons, Aromatic: Method 1501. *NIOSH Man Anal Methods*. **2003**, *127*, 1−7. https://www.cdc.gov/niosh/docs/2003-154/pdfs/ 1501.pdf Accessed May 19, 2018.

(10) NIOSH. Hydrocarbons, halogenated (NIOSH-1003). *NIOSH Man Anal Methods* **2003**, 1−7.

(11) Elskamp, CJ. *OSHA Sampling and Analytical Methods - Toluene (Organic Method #111)*. OSHA Sampling and Analytical Methods. https://www.osha.gov/dts/sltc/methods/organic/org111/org111. pdf. Published 1998. Accessed June 22, 2021.

(12) National Institute for Occupational Safety and Health (NIOSH). Alcohols II: Method1401. *NIOSH Man Anal Methods*. **1994**;(*2*). https://www.cdc.gov/niosh/docs/2003-154/pdfs/1401.pdf. Accessed May 31, 2022

(13) Floyd, E. L.; Sapag, K.; Oh, J.; Lungu, C. T. Photothermal desorption of single-walled carbon nanotubes and coconut shell-activated carbons using a continuous light source for application in air sampling. *Ann Occup Hyg*. **2014**, *58*, 877−888.

(14) Oh, J.; Floyd, E. L.; Watson, T. C.; Lungu, C. T. Fabrication and adsorption characterization of single-walled carbon nanotubes (SWNT) buckypaper (BP) for use in air samples. *Anal. Methods* **2016**, *8*, 4197−4203.

(15) Oh, J.; Floyd, E. L.; Parit, M.; Davis, V. A.; Lungu, C. T. Heat Treatment of Buckypaper for Use in Volatile Organic Compounds Sampling. *J. Nanomater*. **2016**, *2016*, 1.

(16) Shedd, J. S.; Kuehster, W. W.; Ranjit, S.; et al. Determining the Thermal Properties of Buckypapers Used in Photothermal Desorption. *ACS Omega* **2021**, *6*, 5415−5422.

(17) Floyd, E. L.; Oh, J.; Sapag, K.; Oni, T. M.; Shedd, J. S.; Lungu, C. T. Photothermal Desorption of Toluene from Carbonaceous Substrates Using Light Flash. *Nanomaterials* **2022**, *12*, 662.

(18) Jones, S. R.; Shedd, J. S.; Oh, J.; Lungu, C. T. Evaluating the Effects of Modified Windscreens on Organic Vapor Monitor Performance. *Environ Health Insights*. **2022**, *16*, 117863022210784.

(19) Shedd, J. S.; Floyd, E. L.; Oh, J.; Lungu, C. T. FTIR Determination of Surfactant Removal from Arc Discharge Buckypapers for Air Sampling. *J Adv Nanomater*. **2019**, *4*, 11−16.

(20) National Institute for Occupational Safety and Health (NIOSH). *NIOSH Pocket Guide to Chemical Hazards: Toluene*. https://www.cdc. gov/niosh/npg/npgd0619.html. Published 2019. Accessed January 6, 2020.

(21) National Institute for Occupational Safety and Health (NIOSH). *NIOSH Pocket Guide to Chemical Hazards: n-Hexane*. https://www.cdc.

gov/niosh/npg/npgd0322.html. Published 2019. Accessed January 6, 2020.

(22) National Institute for Occupational Safety and Health (NIOSH). *NIOSH Pocket Guide to Chemical Hazards: Trichloroethylene*. https://www.cdc.gov/niosh/npg/npgd0629.html. Published 2019. Accessed January 6, 2020.

(23) National Institute for Occupational Safety and Health (NIOSH). *NIOSH Pocket Guide to Chemical Hazards: Isopropyl Alcohol*. https://www.cdc.gov/niosh/npg/npgd0359.html. Accessed April 18, 2022.

(24) Baseline-Mocon. piD-TECH® eVx User Manual 143-175 *Rev 1*.0. **2000**.

(25) Agilent Technologies. *Agilent 7890B Gas Chromatograph: Data Sheet*. https://www.agilent.com/cs/library/datasheets/public/5991-1436EN.pdf. Published 2013. Accessed January 3, 2022.

(26) Fuller, E. N.; Schettler, P. D.; Giddings, J. C. A new method for prediction of binary gas-phase diffusion coefficients. *Ind. Eng. Chem.* **1966**, *58*, 18−27.

(27) Fuller, E. N.; Ensley, K.; Giddings, J. C. Diffusion of halogenated hydrocarbons in helium. The effect of structure on collision cross sections. *J. Phys. Chem.* **1969**, *73*, 3679−3685.

(28) McDermott, HJ. *Air Monitoring for Toxic Exposures. Second*; John Wiley & Sons: Hoboken, 2004.

(29) Jia, C.; Fu, X. Diffusive Uptake Rates of Volatile Organic Compounds on Standard ATD Tubes for Environmental and Workplace Applications. *Environments* **2017**, *4*, 87.

(30) Poling, BE, Prausnitz, JM. *The Properties of Gases and Liquids*; 5th ed., McGraw-Hill: New York, 2011.

(31) Atkins, P, De Paula, J. *Elements of Physical Chemistry*; 6th ed., W. H. Freeman and Company: New York, 2013.

(32) Pourhakkak, P, Taghizadeh, A, Taghizadeh, M, Ghaedi, M, Haghdoust, S. Fundamentals of adsorption technology. In: *Interface Science and Technology*. Vol *33*. 1st ed. Elsevier Ltd.; 2021:1−70, DOI: 10.1016/B978-0-12-818805-7.00001-1

(33) Gangupomu, R. H.; Sattler, M. L.; Ramirez, D. Comparative study of carbon nanotubes and granular activated carbon: Physicochemical properties and adsorption capacities. *J. Hazard. Mater.* **2016**, *302*, 362−374.

(34) Apul, O. G.; Karanfil, T. Adsorption of synthetic organic contaminants by carbon nanotubes: A critical review. *Water Res.* **2015**, *68*, 34−55.

(35) Kotz, JC, Treichel, PM, Townsend, JR. Intermolecular Forces and Liquids. In: Lockwood, L, ed. *Chemistry and Chemical Reactivity. Eighth*; Brooks/Cole, Cengage Learning: Belmont, 2012:548−581.

(36) 3M Personal Safety Division. *IH Sampling Guide*. (2021). Available at: https://multimedia.3m.com/mws/media/2012971O/ih-sampling-guide.pdf. Accessed June 22, 2021.